

Statistical Analysis of CP-Based Artificial Noise in Narrowband and Broadband PLC Systems

Gustavo M. Campos, Mateus de L. Filomeno, Andrea M. Tonello, and Moisés V. Ribeiro

Abstract—This paper presents a statistical analysis of artificial noise (AN) designed based on the degrees of freedom provided by the cyclic prefix to enhance physical-layer security in power line communication (PLC) systems. A comprehensive description of the AN design is provided, and the AN is modeled as a random vector while its analysis is based on the first- and second-order statistical moments. Numerical results in both narrowband and broadband PLC channels show that, despite being theoretically zero-mean, the expectation may deviate from zero in practice. Moreover, the analysis reveals non-negligible cyclic correlation structures in the AN, which could potentially be exploited by an eavesdropper, thereby compromising the physical-layer security of PLC systems.

Keywords—Artificial noise, physical layer security, power line communication, statistical analysis.

I. INTRODUCTION

Power line communication (PLC) has emerged as a promising solution for data transmission by leveraging the existing power grid infrastructure, thereby enabling ubiquitous and cost-effective connectivity. However, the broadcast nature of PLC systems raises security and privacy concerns, as any device connected to the same electric power grid could potentially intercept the messages. Cryptographic techniques have been used to address this issue; however, they may not be suitable for scenarios involving devices with limited computational resources, such as Internet of Things (IoT). In this context, physical layer security (PLS) emerges as an alternative strategy, exploiting the communication medium's inherent properties to enhance secrecy through diversity in time, frequency, or spatial domains [1].

In single-input single-output (SISO) communication scenarios, PLS has been studied for both PLC and wireless eavesdroppers. For PLC eavesdroppers, measurement-based analysis in [1], [2] and statistical models in [3] show that channel correlation can lead to security breaches. Meanwhile, wireless eavesdropping has been investigated by distinct works [4], [5], examining various metrics and scenarios.

This research was supported in part by Coordenação de Aperfeiçoamento de Pessoal de Nível Superior (CAPES) under Grant 001, Conselho Nacional de Desenvolvimento Científico e Tecnológico (CNPq) under grants 445958/2024-3 and 314741/2020-8, and Fundação de Amparo à Pesquisa do Estado de Minas Gerais (FAPEMIG) under grant APQ-04623-22.

Gustavo M. Campos, Mateus de L. Filomeno, and Moisés V. Ribeiro are with the Electrical Engineering Department, Federal University of Juiz de Fora (UFJF), Juiz de Fora, MG 36036-900, Brazil, (e-mail: gustavo.moraes@estudante.ufjf.br, delimafilomeno@gmail.com, moises.ribeiro@ufjf.br).

Andrea M. Tonello is with the Institute of Networked and Embedded Systems, Alpen-Adria University Klagenfurt, 9020 Klagenfurt, Austria (e-mail: andrea.tonello@aau.at).

Overall, the literature emphasizes the need to advance PLS to meet security requirements.

In light of this, since the idea of PLS is to grant the legitimate receiver a greater capacity than the eavesdropper, a practical approach to accomplish this is the injection of artificial noise (AN). Shafie *et al.* [6] proposed an AN-assisted scheme to improve communication security against intruders by exploiting any degree of uncorrelation between PLC and wireless channels. Similarly, the authors in [7] studied AN injection in PLC networks, showing its effectiveness in mitigating the negative impact of PLC eavesdroppers. Nevertheless, the former approach demands higher computational complexity, while the latter relies on a complex cooperative scheme with reduced spectral efficiency.

Otherwise, Qin *et al.* [8] proposed a simpler alternative AN generation. The authors, considering a SISO-orthogonal frequency-division multiplexing (OFDM) system, have exploited the degrees of freedom introduced by the cyclic prefix (CP) to design the AN. This idea was further explored in [9], where the authors showed that the AN power is mainly concentrated within the CP duration, leading to higher peak-to-average power ratio (PAPR). Filomeno *et al.* [10] subsequently analyzed this technique in PLC system in the presence of both PLC and wireless eavesdroppers, revealing reasonable effectiveness against near PLC eavesdroppers. Since the AN lies in the null space of a multipath legitimate channel, the resulting AN samples may exhibit correlation. This correlation, while essential for preserving legitimate communication, could potentially be exploited by an eavesdropper to estimate and mitigate the AN impact [11]—an aspect that, to the best of our knowledge, has not been thoroughly investigated in the literature.

Although this AN has already been studied in previous works, its statistical properties remain largely unexplored, particularly in the PLC context. To address this research gap, this paper conducts a statistical analysis of AN when narrowband and broadband PLC systems are considered. In this work, we model the AN as a random vector and characterize it through its first- and second-order moments. Specifically, we analyze its expectation vector and autocorrelation matrix. This analysis cover the frequency bands 9 – 500 kHz (narrowband) and 1.7 – 86 MHz (broadband), allowing us to determine whether the observed behavior can be exploited by malicious nodes.

Notation: $\mathbb{E}\{\cdot\}$ denotes the expectation operator, while $(\cdot)^T$ and $(\cdot)^\dagger$ denote the transpose and Hermitian operators, respectively. Furthermore, $\mathbf{0}_{c \times d}$ stands for an $(c \times d)$ -size matrix of zeros, whereas \mathbf{I}_c is a c -size identity matrix.

II. PROBLEM FORMULATION

We consider a discrete-time wiretap channel model [10], in which a legitimate transmitter, namely Alice, sends confidential information to a legitimate receiver, called Bob, while a malicious eavesdropper, referred to as Eve, seeks to intercept and overhear the confidential information. The data communication system is based on a CP-based transmission system, where a CP is appended to each transmitted block to accommodate intersymbol interference (ISI) and facilitate frequency domain equalization. In this system, different digital modulation schemes may be employed, such as multicarrier (OFDM), multi-chirp (orthogonal chirp-division multiplexing (OCDM)), or single-carrier single carrier with cyclic prefix (SC-CP).

In the considered discrete-time model, we assume that Alice and Bob communicate through a linear time-invariant PLC channel corrupted by the presence of additive noise. The receiver is assumed to be perfectly synchronized. As is typical for wired communication systems, baseband transmission is required in PLC, which implies that the transmitted block symbols must be real-valued. In this context, let $\mathbf{x}'_i \in \mathbb{R}^{N \times 1}$ denote the vector representation of the i^{th} transmitted information block in the discrete-time domain. After CP insertion, the vector representation of the real-valued transmitted information block is given by

$$\mathbf{x}_i = \Psi_T \mathbf{x}'_i, \quad (1)$$

where the matrix $\Psi_T = [\mathbf{E}_{N_{cp} \times N}^T \mathbf{I}_N]^T$ is responsible for the CP insertion, with N_{cp} indicating the CP-length and $\mathbf{E}_{N_{cp} \times N} = [\mathbf{0}_{N_{cp} \times (N-N_{cp})} \mathbf{I}_{N_{cp}}]$.

Alice sends the information block \mathbf{x}_i along with a AN random vector (block) $\mathbf{a}_i \in \mathbb{R}^{(N+N_{cp}) \times 1}$. The overall built block, i.e., information plus AN, is transmitted through a linear and time-invariant broadcast channel, reaching Bob and Eve, denoted, respectively, by “b” and “e”. For baseband transmission, the channel can be described by a Toeplitz matrix $\mathbf{H}^l \in \mathbb{R}^{(N+N_{cp}) \times (N+N_{cp})}$, where $l \in \{b, e\}$. Then, at the l^{th} user, the vector representation for the i^{th} received block can be written as

$$\mathbf{y}_i^l = \mathbf{H}^l(\mathbf{x}_i + \mathbf{a}_i) + \mathbf{w}_i^l, \quad \forall l \in \{b, e\}, \quad (2)$$

in which $\mathbf{w}_i^l \in \mathbb{R}^{(N+N_{cp}) \times 1}$ indicates the additive noise vector affecting the i^{th} block and l^{th} user.

Next, the l^{th} user removes the CP from \mathbf{y}_i^l , eliminating ISI and converting the linear channel convolution into a circular one, resulting in a circulant channel matrix. The vector representation of the i^{th} block received by the l^{th} user is expressed as

$$\begin{aligned} \mathbf{y}'_i^l &= \Psi_R \mathbf{y}_i^l \\ &= \Psi_R \mathbf{H}^l \mathbf{x}_i + \Psi_R \mathbf{H}^l \mathbf{a}_i + \Psi_R \mathbf{w}_i^l \end{aligned} \quad (3)$$

with the matrix $\Psi_R = [\mathbf{0}_{N \times N_{cp}} \mathbf{I}_N]$ being responsible for the CP removal.

From (3) we see an additional noise term associated with the AN is received by the l^{th} user, i.e., $\Psi_R \mathbf{H}^l \mathbf{a}_i$. In this regard, Alice aims to design the AN such that it degrades Eve’s signal-to-noise-ratio (SNR) while having a negligible

impact on Bob’s detection performance. To achieve this, Alice must design \mathbf{a}_i so that its convolution with Bob’s channel impulse response (CIR) yields a null signal, which should not occur regarding Eve’s. Building on this concept, the authors of [8] exploited the degrees of freedom introduced by the CP, therefore using the matrix $\Psi_R \mathbf{H}^b \in \mathbb{R}^{N \times (N+N_{cp})}$. This technique allows \mathbf{a}_i to be represented as

$$\mathbf{a}_i = \mathbf{V}_{\text{null}}^b \mathbf{d}_i, \quad (4)$$

such that $\mathbf{d}_i \in \mathbb{R}^{N_{cp} \times 1}$ is a vector of independent Gaussian random variables and $\mathbf{V}_{\text{null}}^b \in \mathbb{R}^{(N+N_{cp}) \times N_{cp}}$ defines the right null space of $\Psi_R \mathbf{H}^b$, i.e.,

$$\Psi_R \mathbf{H}^b \mathbf{V}_{\text{null}}^b = \mathbf{0}_{N \times N_{cp}}. \quad (5)$$

Hence, to design \mathbf{a}_i , Alice needs to obtain the CIR of Bob, which can be accomplished, for instance, via a feedback channel. Then, using this channel information, the matrix \mathbf{H}^b is constructed, and $\mathbf{V}_{\text{null}}^b$ is computed via singular value decomposition (SVD). Finally, the vector \mathbf{d}_i can be generated using a discrete random variable generator.

Since the AN vector \mathbf{a}_i is constructed using (4), its statistical properties are determined by the structure of $\mathbf{V}_{\text{null}}^b$. Although the vector \mathbf{d}_i comprises uncorrelated random variables, the transformation applied by $\mathbf{V}_{\text{null}}^b$ can introduce significant correlation among the elements of \mathbf{a}_i . This induced correlation may weaken the effectiveness of the AN, potentially allowing Eve to exploit its structure to mitigate its disruptive impact. To assess this vulnerability, the following sections analyze the AN as a random vector through its first- and second-order statistics.

III. ANALYSES OF THE CP-BASED AN AS A RANDOM VECTOR

The AN can be modeled as a random vector onto the null space of Bob’s CIR. To analyze its statistical properties, we consider its first- and second-order moments, i.e., the expectation vector and autocorrelation matrix. In this context, we represent the random vector through its sample functions observed over time. Specifically, let \mathbf{a}_i denote the i^{th} sample function (i.e., realization) of the AN random vector, corresponding to the AN generated during the i^{th} transmission block. Thus, the temporal evolution of this random vector is captured by the set of vectors $\{\mathbf{a}_i\}$, which enables its statistical analysis across multiple time instants.

A. Expectation of a Random Vector

The expectation of a random vector is given by

$$\boldsymbol{\mu}_a = \mathbb{E}_i\{\mathbf{a}_i\}. \quad (6)$$

Although the PLC channel is inherently random and slowly time-varying, its null-space $\mathbf{V}_{\text{null}}^b$ is treated as deterministic. This holds under the assumption that the AN generation occurs within the coherence time of the PLC channel, during which its properties and characteristics remain invariant. Therefore,

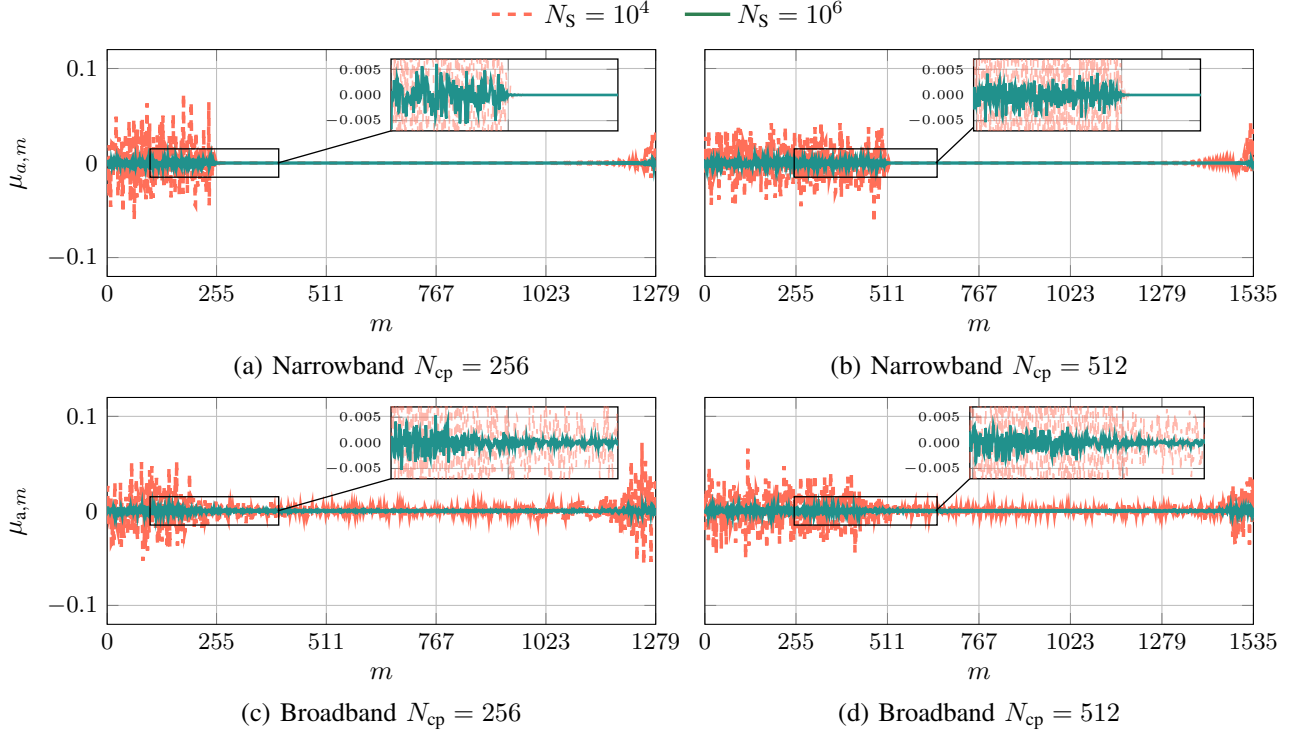


Fig. 1. Expectation of the AN for the narrow and broadband PLC channels, computed over different realizations and N_{cp} values. In this figure, $\mu_a[m]$ represents the m^{th} element of μ_a .

the expectation of the considered AN random vector can also be expressed as

$$\begin{aligned}\mu_a &= \mathbb{E}_i\{\mathbf{V}_{\text{null}}^b \mathbf{d}_i\} \\ &= \mathbf{V}_{\text{null}}^b \mathbb{E}_i\{\mathbf{d}_i\}.\end{aligned}\quad (7)$$

If \mathbf{d}_i is a zero mean random vector, i.e., $\mathbb{E}_i\{\mathbf{d}_i\} = \mathbf{0}_{N_{cp} \times 1}$, then one has

$$\mu_a = \mathbf{0}_{(N+N_{cp}) \times 1}. \quad (8)$$

This result sets the stage for the evaluation of the autocorrelation matrix.

B. Autocorrelation Matrix of a Random Vector

The autocorrelation matrix of a random vector is a deterministic function that quantifies the temporal dependence between elements of the AN random vector at different lags. It is expressed as

$$\mathbf{R}_{aa} = \mathbb{E}_i\{\mathbf{a}_i \mathbf{a}_i^\dagger\}, \quad (9)$$

which is a symmetric and positive semi-definite matrix. Substituting (4) in (9), results in

$$\begin{aligned}\mathbf{R}_{aa} &= \mathbb{E}_i\left\{(\mathbf{V}_{\text{null}}^b \mathbf{d}_i)(\mathbf{V}_{\text{null}}^b \mathbf{d}_i)^\dagger\right\} \\ &= \mathbf{V}_{\text{null}}^b \mathbb{E}_i\{\mathbf{d}_i \mathbf{d}_i^\dagger\} \mathbf{V}_{\text{null}}^{b\dagger},\end{aligned}\quad (10)$$

in which $\mathbb{E}\{\mathbf{d}_i \mathbf{d}_i^\dagger\} = \mathbf{\Lambda}_{\sigma_d^2}$, $\forall i$, is a diagonal matrix that stands for the correlation matrix of the AN, leading to

$$\mathbf{R}_{aa} = \mathbf{V}_{\text{null}}^b \mathbf{\Lambda}_{\sigma_d^2} \mathbf{V}_{\text{null}}^{b\dagger}. \quad (11)$$

The knowledge of (8) states that the autocorrelation and autocovariance matrices are equal. Thus, to obtain the

correlation between the elements of AN random vector, we use the correlation index, which is given by

$$\rho_{aa}[m, n] = \frac{R_{aa}[m, n]}{\sqrt{R_{aa}[m, m] R_{aa}[n, n]}}, \quad (12)$$

$\forall m, n \in \{0, 1, \dots, N + N_{cp} - 1\}$, in which $R_{aa}[m, n]$ is the correlation between m^{th} and n^{th} elements. By definition, $-1 \leq \rho_{aa}[m, n] \leq 1$.

From the main diagonal of the matrix \mathbf{R}_{aa} , we can also define a vector $\mathbf{v}_{\sigma_a^2}$ that represents the variances of the AN random vector $\{\mathbf{a}_i\}$, i.e.,

$$\mathbf{v}_{\sigma_a^2} = [v_{\sigma_a^2, 0}, v_{\sigma_a^2, 1}, \dots, v_{\sigma_a^2, N+N_{cp}-1}]^T \quad (13)$$

in which $v_{\sigma_a^2, m} = R_{aa}[m, m]$.

Section IV offers an initial statistical analysis of the CP-based AN as a random vector for both narrowband and broadband PLC channels.

IV. NUMERICAL RESULTS

This section numerically evaluates and analyzes the expectation vector and autocorrelation matrix. In this sense, two distinct PLC bandwidths are considered: narrowband (9–500 kHz) and broadband (1.7–86 MHz). In the broadband case, the Alice-Bob PLC CIR used for AN generation is obtained from the dataset obtained from the measurement campaign detailed in [12]. As for the narrowband case, the PLC CIR is based on the multi-path channel model described in [13]; the parameters for this model are taken from the IEEE 1901.2 Standard [14].

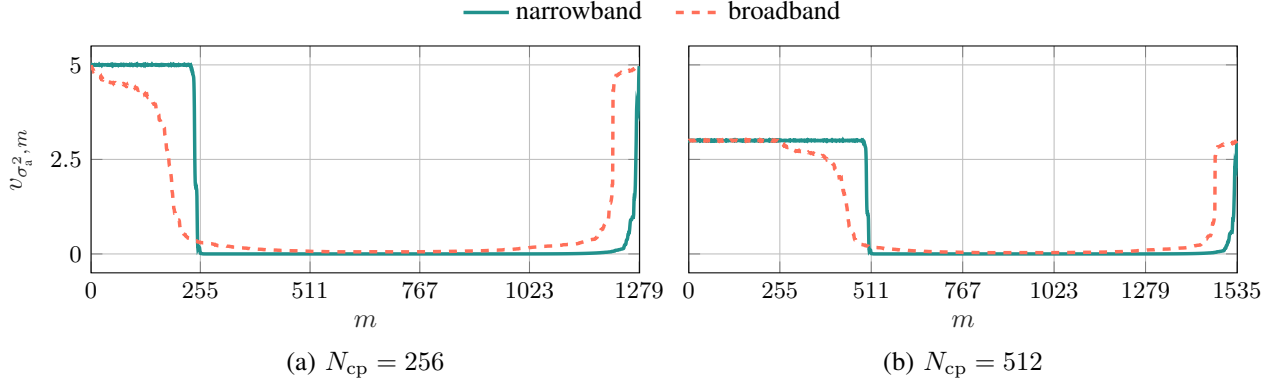


Fig. 2. Variance of the AN for the narrow and broadband PLC channels, computed over $N_S = 10^6$ realizations and evaluated under different values of N_{cp} . In this figure, $v_{\sigma_a^2}[m]$ denotes the m^{th} element of the vector $\mathbf{v}_{\sigma_a^2}$.

For the statistical analysis, the AN random vector \mathbf{d}_i is generated assuming $i \in \{1, \dots, N_S\}$, with $N_S \in \{10^4, 10^6\}$. In addition, $N = 1024$ and $N_{cp} \in \{256, 512\}$ are assumed. The expectation vector and autocorrelation matrix are computed based on (6) and (9), respectively. To do so, the expectation operator is performed by a conventional unbiased sample mean estimator, and the autocorrelation matrix is obtained from an unbiased covariance estimator over the N_S realizations of the AN random vector because such realizations are independent and identically distributed.

Fig. 1 illustrates the vector $\mu_a[m]$, which is an unbiased estimate of the expectation vector as a function of the sample index m , for $N_S = 10^4$ and $N_S = 10^6$. Figs. 1(a) and (b) show the narrowband PLC channel with $N_{cp} = 256$ and $N_{cp} = 512$, respectively, whereas Figs. 1(c) and (d) show the corresponding estimates for the broadband PLC channel. In both narrowband and broadband PLC channels, the expectation vector exhibits pronounced non-zero values throughout the CP interval, especially for $N_S = 10^4$. This is more prominent for the narrowband scenario because its CIR concentrates energy into a few highly correlated CP taps, unlike the broadband channel's diffuse multipath, a contrast further highlighted by the use of a modeled versus a measured CIR. For $N_S = 10^6$, although a small deviation still persists within the CP length, the expectation vector converges much closer to zero for all elements of the AN random vector for both narrowband and broadband PLC channels.

The difference between the results for $N_S = 10^4$ and $N_S = 10^6$ indicates that, although a zero-mean random vector can theoretically be modeled as a zero-mean random vector, its behavior in practice may differ. The reason behind this result lies in the variance differences among the random variables that compose the random vector, as illustrated in Fig. 2. Note that the variance of the AN random vector is higher throughout the CP length for all investigated cases and types of PLC channels. In particular, this variance disparity points to a significant energy distribution variation across the AN random vector, which also contributes to its high PAPR, as previously pointed out by [9].

The analysis of the autocorrelation matrix of the AN random vector is carried out for $N_S = 10^6$. Figs. 3(a)

to (d) show the heatmaps of the correlation matrices for $N_{cp} = 256$ and $N_{cp} = 512$, considering both narrowband and broadband PLC channels. For the narrowband PLC channel, Fig. 3(a) shows that the autocorrelation matrix remains identically zero for all lags within the CP duration, but beyond this region, off-diagonal elements exhibit cyclic alternations between low and high correlation values. A similar behavior is observed in Fig. 3(b) for the longer CP ($N_{cp} = 512$), with an extended initial zero-correlation region corresponding to the increased CP duration. Changing the analyses to the broadband PLC channel, displayed in Figs. 3(c) and (d), the zero-correlation region is less distinct, though still visible for $N_{cp} = 512$ —see Fig. 3(d). Notably, although less visually apparent, both autocorrelation matrices for broadband PLC channels exhibit high-magnitude correlation values that recur in a cyclic pattern. These correlation characteristics may pose a security vulnerability, as their structured and persistent nature could allow Eve to develop advanced signal processing countermeasures, such as the one discussed in [11] and the references contained therein, against the AN-based protection.

V. CONCLUSIONS

This paper has characterized the AN random vector, designed based on the degrees of freedom introduced by the CP, for narrow and broadband PLC channels. In this regard, the characterization was conducted over the first- and second-order moments of the AN random vector. Our analysis shows that, despite being theoretically modeled as a zero-mean random vector, the AN may exhibit different characteristics in practice, particularly within the CP region. Also, the analysis of the correlation matrices shows that the AN exhibits significant correlation values for lags beyond the CP length, with distinct patterns depending on the PLC channel and CP length. These results indicate that the AN random vectors, generated based on the degrees of freedom introduced by the CP, should be further investigated to prevent the eavesdropper from estimating and mitigating its impact, which would compromise the PLS objectives. As future work, we mention the statistical analysis of the signal observed by Eve, along with the investigation of possible countermeasures she could employ to suppress the AN.

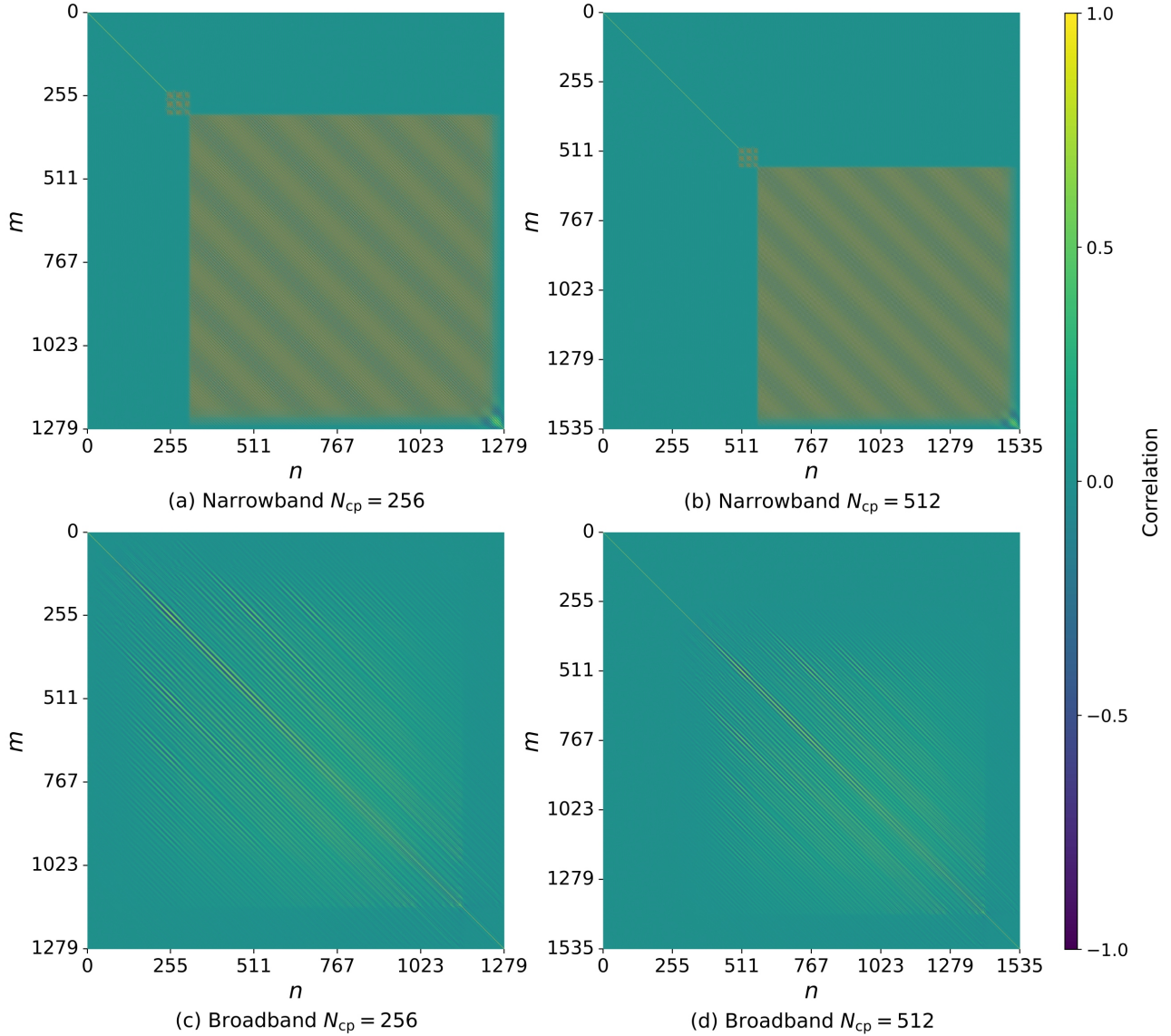


Fig. 3. Heatmap of the correlation matrix of the AN for the narrow and broadband PLC channels, considering different values of N_{cp} .

REFERENCES

- [1] A. Pittolo and A. Tonello, "Physical layer security in power line communication networks: An emerging scenario, other than wireless," *IET Commun.*, vol. 8, pp. 1239–1247, May 2014.
- [2] Á. Camponogara, H. V. Poor, and M. V. Ribeiro, "Physical layer security of in-home PLC systems: Analysis based on a measurement campaign," *IEEE Syst. J.*, vol. 15, no. 1, pp. 617–628, Mar. 2021.
- [3] V. Mohan, A. Mathur, V. Aishwarya, and S. Bhargav, "Secrecy analysis of PLC system with channel gain and impulsive noise," in *Proc. IEEE Veh. Technol. Conf.*, 2019, pp. 1–6.
- [4] Á. Camponogara, H. V. Poor, and M. V. Ribeiro, "PLC systems under the presence of a malicious wireless communication device: Physical layer security analyses," *IEEE Syst. J.*, vol. 14, no. 4, pp. 4901–4910, Dec. 2020.
- [5] Á. Camponogara, R. D. Souza, and M. V. Ribeiro, "The effective secrecy throughput of a broadband power line communication system under the presence of colluding wireless eavesdroppers," *IEEE Access*, vol. 10, pp. 85 019–85 029, 2022.
- [6] A. El Shafie, M. F. Marzban, R. Chabaan, and N. Al-Dhahir, "An artificial-noise-aided secure scheme for hybrid parallel PLC/wireless OFDM systems," in *Proc. IEEE Int. Conf. Commun.*, 2018, pp. 1–6.
- [7] A. Salem, K. A. Hamdi, and E. Alsusa, "Physical layer security over correlated log-normal cooperative power line communication channels," *IEEE Access*, vol. 5, pp. 13 909–13 921, 2017.
- [8] H. Qin *et al.*, "Power allocation and time-domain artificial noise design for wiretap OFDM with discrete inputs," *IEEE Trans. Wirel. Commun.*, vol. 12, no. 6, pp. 2717–2729, June 2013.
- [9] F. Yang, K. Zhang, Y. Zhai, J. Quan, and Y. Dong, "Artificial noise design in time domain for indoor SISO DCO-OFDM VLC wiretap systems," *J. Lightw. Technol.*, vol. 39, no. 20, pp. 6450–6458, Oct. 2021.
- [10] M. de L. Filomeno, G. M. Campos, Á. Camponogara, P. H. Sartorello, and M. V. Ribeiro, "Artificial noise for in-home PLC networks under the presence of PLC and wireless eavesdroppers," in *Symp. Internet Things*, Oct. 2023, pp. 1–5.
- [11] K. R. Duffy and M. Médard, "Soft detection physical layer insecurity," in *IEEE Glob. Commun. Conf.*, 2023, pp. 1747–1752.
- [12] M. S. P. Facina, H. A. Latchman, H. V. Poor, and M. V. Ribeiro, "Cooperative in-home power line communication: Analyses based on a measurement campaign," *IEEE Trans. Commun.*, vol. 64, no. 2, pp. 778–789, Feb. 2016.
- [13] M. Zimmermann and K. Dostert, "A multipath model for the powerline channel," *IEEE Trans. on Commun.*, vol. 50, no. 4, pp. 553–559, Apr. 2002.
- [14] "IEEE Standard for low-frequency (less than 500 khz) narrowband power line communications for smart grid applications," *IEEE Std 1901.2-2013*, pp. 1–269, 2013.